Geant4-BASED OPTICAL PHOTON DISTRIBUTION MODELING IN A SEGMENTED SILICON-PHOTOMULTIPLIER SCINTILLATOR DETECTOR FOR THE RECOIL FILTER DETECTOR OPTIMIZATION*

C. Hiver [a], M. Matejska-Minda [b], D. Duda[b]
P.J. Napiorkowski[a], P. Bednarczyk[b], P. Kulessa[b]
B. Sowicki[b], M. Zięblński[b]

[a]Heavy Ion Laboratory, University of Warsaw, 02-093 Warszawa, Poland
[b]Institute of Nuclear Physics Polish Academy of Sciences, 31-342 Kraków, Poland

Received 27 November 2025, accepted 26 January 2026, published online 31 March 2026

Geant4 simulations were performed to investigate the scintillation light distribution in a segmented Silicon-Photomultiplier (SiPM) based detector module, which is currently being developed for the upgraded Recoil Filter Detector (RFD). The goal is to replace conventional photomultiplier tubes (PMTs), whose performance degrades under high secondary electron rates, with SiPM arrays coupled to ultra-thin plastic scintillators. Two scintillator types (EJ-228 and EJ-214) and a 4×4 SiPM matrix were modeled, including detailed optical properties and interface definitions. Simulations of 20 keV secondary electron bunches show that for scintillator thicknesses up to about 25 μm, the generated light remains highly localized and is collected almost entirely by a single SiPM cell. The results show that the expected improvement in counting capability is possible thanks to detector segmentation, and provide guidance for the optimal design of future RFD modules.

DOI:10.5506/APhysPolBSupp.19.1-A30

1. Introduction

The Recoil Filter Detector (RFD) [1] is an ancillary device designed to measure the time-of-flight (ToF) of evaporation residues in coincidence with γ rays. By providing precise information on the recoil ToF and emission angle, the RFD enables significant improvement of γ-ray spectra (Doppler

* Presented at the XXXVIII Mazurian Lakes Conference on Physics, Piaski, Poland, August 31–September 6, 2025.

correction and background suppression). The detector consists of 18 individual sensors. Each sensor produces several hundred of secondary electrons (SE) by heavy ions passing through a thin Mylar foil, which are accelerated and focused by a 20 keV electrostatic lens onto a thin plastic scintillator.

The RFD was successfully used in a variety of experiments [1–5]. However, several limitations have affected its heavy-ion detection capabilities. The high counting rates — primarily caused by beam scattering — led to aging of the photomultiplier tubes (PMTs), resulting in performance degradation during operations. Hence, new sensor modules based on Silicon Photomultipliers (SiPMs) [6] are considered to mitigate these issues: SiPMs enable increased segmentation of the sensitive area, improving the detector's capability to operate under high SE rates. A new version of the RFD for the EAGLE array at HIL UW [7] is currently under development, including the integration of fast plastic scintillators coupled to the segmented SiPM arrays.

This article presents the simulations performed with the Geant4 toolkit, modeling light propagation induced by an SE beam in an ultra-thin scintillator film coupled to a segmented SiPM matrix. The goal of the study is to determine the light-spot size and intensity distribution generated by the SE beam in order to identify the optimal segmentation of the SiPM matrix for each RFD module.

2. Geant4 simulations

For the RFD, the scintillator must be thick enough to ensure complete absorption of 20 keV electrons, which have a range of about 6 μm in a typical plastic scintillator, while being as thin as possible to minimize sensitivity to γ rays. Two types of plastic scintillators are under investigation: a 50 μm EJ-228 film [8] and a 25 μm EJ-214 film [9] — the thinnest commercially available for each type. A homogeneous scintillator layer is placed on top of a SiPM array, separated from it by a thin layer of optical grease.

A 4×4 onsemi SiPM array (MicroFJ-30035-TSV [10]) was selected. Each 3.16×3.16 mm^2 SiPM cell contains 5676 single-photon avalanche diodes (SPADs) of 35 μm pitch, yielding a micro-cell fill factor of 75% over an active area of 3.07×3.07 mm^2. The device exhibits peak spectral sensitivity around 420 nm. Each SiPM element is made of four layers: a coating protecting the glass cap (a few micrometers of composite plastic), a glass cap (370 μm of borosilicate-like glass), a layer of optical glue (a few micrometers of composite plastic), and the silicon substrate (90 μm of silicon).

The scintillation process and optical photon transportation were modeled with the Geant4 [13–15] toolkit, implemented with the standard FTFP_BERT physics list together with G4EmLivermorePhysics (in place of G4EmStandard Physics) and the additional G4OpticalPhysics. The chemical composition

and optical properties of each component were explicitly implemented, with parameters as listed in Table 1. Simulations allow for an unlimited number of interactions of the particles in the scintillator to preserve a good accuracy.

Table 1. Optical properties for EJ-228 and EJ-214 scintillators and other components of the individual RFD sensor (for 400 nm wavelength, according to Refs. [11, 12]). GC stands for Glass Coating.

Scintillator	EJ-228	EJ-214	GC	Glass	Glue	Si
Emission peak [nm]	390	435				
Refractive index	1.59	1.58	1.5	1.54	1.5	5.62
Absorption length [cm]	120	120	120	300	120	N/A
Scintillation yield [MeV^{-1}]	10200	9000				
Decay time [ns]	2	1.2				

Accurate modeling of light propagation in such a complex system requires proper treatment of optical interfaces between neighboring materials. In the Geant4 "unified" surface model [16], an interface is defined by the types of the adjacent materials (dielectric, metal, or coating), the surface finish (polished or ground), and the surface roughness, parametrized by the mean micro-facet angle σ_α (relevant for ground surfaces only). The optical interfaces used in the simulation are summarized in Table 2.

Table 2. Main optical interfaces between the components of the RFD sensor.

Interface	Type	Finish	σ_α
Vacuum–scintillator	Dielectric–dielectric	Ground	0.5
Scintillator–coating	Dielectric–dielectric	Ground	0.5
Coating–glass	Dielectric–dielectric	Ground	0.1
Glass–glue	Dielectric–dielectric	Ground	0.1
Glass–vacuum	Dielectric–dielectric	Polished	N/A
Glue–silicon	Dielectric–dielectric	Ground	0.1

Table 1 shows only the average emission peak and scintillation yield, however, a realistic emission curve have been used to generate scintillation photons. Additionally, a realistic Photon Detection Efficiency (PDE) has been implemented for counting the number of photons reaching each cell and actually triggering a signal.

3. Results

This study focuses on the response of the detector to the signal of interest: a SE beam generated by ions passage through the Mylar foil. The geometry of the RFD ensures that the scintillators do not directly view the target position, thereby protecting them against other unwanted radiation.

The range of 20 keV electrons in a plastic scintillator is only a few micrometers. A well-focused SE beam deposits its energy within a very small volume, which can be treated as a point-like source of scintillation light. The resulting illumination pattern on the SiPM array is shown in Fig. 1 (left), while Fig. 1 (right) presents a side and a zoomed views. Most of the emitted light is absorbed by the SiPM cell directly facing the interaction point.

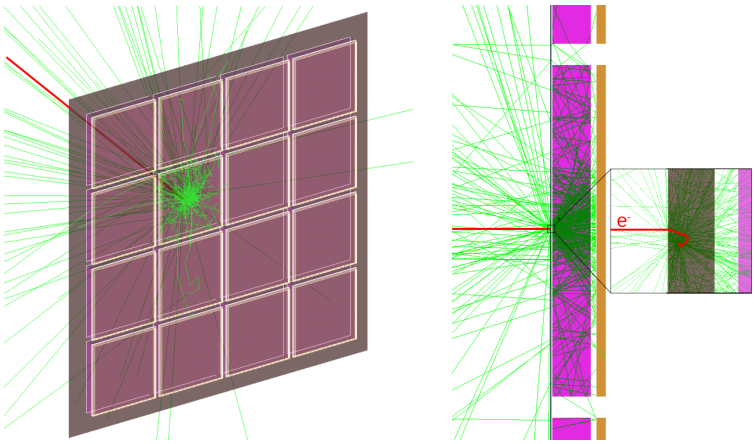

Fig. 1. (Color online) Geant4 simulation of scintillation light produced by a single 20 keV electron in a 25 μm-thick EJ-214 plastic scintillator. The scintillation photons are displayed in green, the incoming electron in red. Left: Isometric view of the scintillator (brown) and the array of 16 SiPMs. Right: Side and zoomed views of the module. The glass cap is shown in pink and the silicon substrate in beige, while the glass coating and the optical grease layer are depicted as transparent.

To study the influence of the scintillator thickness on the light distribution, simulations were performed for scintillator layers with thicknesses between 10 μm and 5 mm. The results are shown in Fig. 2. For the thinnest layers, nearly all photons are detected in a single SiPM cell. As the scintillator becomes thicker, the light spreads over several cells, and for a 5 mm-thick scintillator, the entire SiPM array is illuminated. Similar simulations performed for EJ-228 show nearly identical light-distribution patterns, indicating that both scintillator types behave equivalently within the studied geometry.

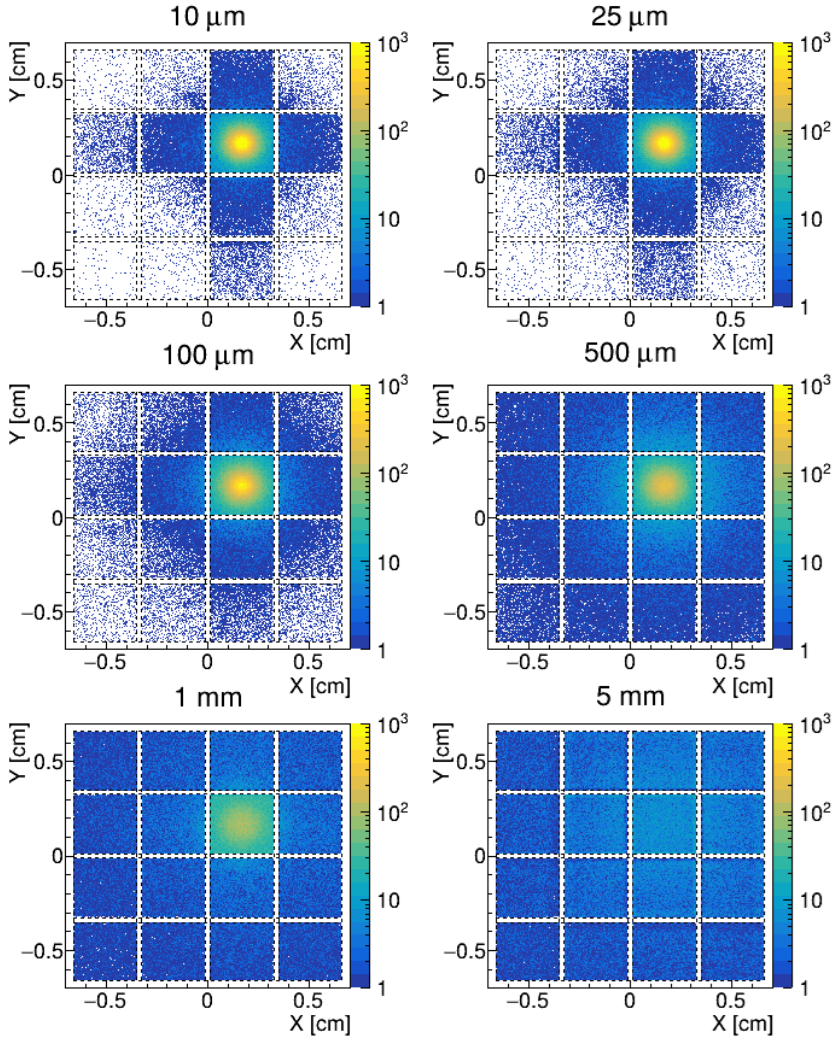

Fig. 2. Distribution of scintillation photons detected by the SiPM matrix for various EJ-214 scintillator thicknesses, based on a simulation of 100 bunches of 400 electrons at 20 keV. Thin dashed lines mark the boundary of each 16 of the individual cells.

For a 25 μm-thick layer, on average, only 150 to 200 photons are detected in each neighboring cell, compared to over 21,000 photons being absorbed in the central cell facing the beam. These results indicate that a thickness of approximately 25 μm represents the upper limit at which the response remains effectively confined to a single SiPM cell.

4. Conclusion

The Geant4 simulations demonstrate that the counting-rate capability of each detection module of the RFD (Mylar foil + focusing lens + scintillator) can be significantly increased by replacing the previous PMTs with SiPM arrays. Coupling a 4×4 SiPM matrix to ultra-thin plastic scintillators enables segmentation of the sensitive area and thus the possibility of improving the counting rate by up to a factor of 16, provided that the secondary electron beam is well focused and scintillation light is not shared between neighboring cells. In the simulations, typical bunches of 400 secondary electrons with a kinetic energy of 20 keV were used to irradiate 25 μm EJ-214 and 50 μm EJ-228 plastic scintillator. The results show that for both scintillators, the vast majority of the generated scintillation light is collected by the SiPM cell directly facing the interaction point, confirming the expected enhancement in the counting-rate performance of each RFD element. As a next step, the results will be compared with real data from available sources and, subsequently, in-beam data.

This work is supported by the National Science Centre (NCN), Poland, under the SONATA BIS-13 grant agreement No. 2023/50/E/ST2/00621.

REFERENCES

[1] W. Męczyński *et al.*, *Nucl. Instrum. Methods Phys. Res. A* **580**, 1310 (2007).
[2] M. Matejska-Minda *et al.*, *Phys. Rev. C* **100**, 054330 (2019).
[3] M. Lach *et al.*, *Eur. Phys. J A* **16**, 309 (2003).
[4] D. Rodrigues *et al.*, *Phys. Rev. C* **92**, 024323 (2015).
[5] P. Bednarczyk *et al.*, *Eur. Phys. J A* **20**, 45 (2003).
[6] F. Acerbi *et al.*, *Nucl. Instrum. Methods Phys. Res. A* **926**, 16 (2019).
[7] M. Matejska-Minda *et al.*, *Acta Phys. Pol. B Proc. Suppl.* **18**, 2A-42 (2025).
[8] https://eljentechnology.com/products/plastic-scintillators/ej-228-ej-230
[9] https://eljentechnology.com/products/plastic-scintillators/ej-214
[10] https://www.onsemi.com/pdf/datasheet/arrayj-series-d.pdf
[11] M.N. Polyanskiy, *Sci. Data* **11**, 94 (2024)
[12] https://fr.scribd.com/document/662500932/schott-optical-glass-datasheet-collection-en
[13] S. Agostinelli *et al.*, *Nucl. Instrum. Methods Phys. Res. A* **506**, 250 (2003).
[14] J. Allison *et al.*, *IEEE Trans. Nucl. Sci.* **53**, 270 (2006).
[15] J. Allison *et al.*, *Nucl. Instrum. Methods Phys. Res. A* **835**, 186 (2016).
[16] A. Levin, Ch. Moisan, *IEEE Nucl. Sci. Symp.* **2**, 706 (1996).